International Journal of Nanoelectronics and Materials

In Press, Accepted Manuscript – Note to users

First principles enhanced electronic band structure of $SrTiO_3$ using DFT+U method

[1, 2, a)] Akeem Adekunle Adewale [1,b)]Abdullah Chik

[1]School of Materials Engineering, Universiti Malaysia Perlis (UniMAP), 02600 Arau, Jejawi, Perlis, Malaysia.

[2]Department of Physics and Materials science, Kwara State University, Malete, Kwara state, Nigeria

[a)] Corresponding author: adewaleakeem12@gmail.com

[b)] abdullahchik@unimap.edu.my

Abstract

Density functional theory (DFT) technique was used to study the influence of Hubbard U on the calculated electronic properties of perovskite $SrTiO_3$. We used the Quantum Espresso (QE) software package with exchange-correction energy function within local density approximation for DFT and DFT+U calculations. The band structure, total and partial density of states (DOS and PDOS) were calculated. Three set of methods were adopted in the calculations: DFT without U, DFT+U with calculated U through linear response theory, and DFT+U with manually increment of U value. The calculated Hubbard U using linear response theory is 3.27 while selected U for manual increment method were chosen from 4.27 to 10.27 with an interval of 1. For DFT and DFT+U with calculated U, the calculated band gap were 1.80 and 2.19 eV respectively. During increasing of U, the calculated band gap were increasing from 2.43 eV (@U=4.27) and reaches peak of 3.06 eV (@U=8.27) which later reduce to 2.19 eV (@U=10.27). Therefore, DFT+U method with incremental Hubbard U resulted in better band gap value of 3.06eV that is closer to the experimental result of 3.25eV.

Keywords

$SrTiO_3$, QE, energy band gap, density of state, Hubbard-U parameter, DFT, DFT+U

1.0 Introduction

DFT + Hubbard U (DFT +U) is a method which aims to correct limitations of density functional theory (DFT) calculation especially in electronic properties [1]. Among several

exchange-correlation energy functions in DFT calculation; Local density approximation (LDA) and generalized gradient approximation (GGA) [2] are the common function use in calculation of band gap for semiconductors and insulators [3,4] but they mostly underestimate the band gap value and cast doubt on results of transition point of the material [4,5]. In the DFT +U approach, energy band gap of most materials can be improved by varying the *U* parameter [6,7]. The DFT+U methods has been explored by Kinaci, Sevik, & Çağın, (2010) using $SrTiO_3$ and found band gap improved with DFT +U; at U= 3.2 and 5, the band gap were 2.026 and 2.351 eV respectively.

$SrTiO_3$ (STO), a transition metal oxides, is a perovskite oxide with a crystalline cubic structure at room temperature and tetragonal structure (phase transition) at 105 K [8,9]. Recently, STO draws attention of numerous researchers because of its applications in ferroelectric, electroconductive, and photovoltaic devices. However, the knowledge of electronic properties (band structure, electronic structure and density of state) of materials is essential for the development of new applications. Several literature had reported the structural, dielectric [10], optical [11], infrared [12] and as well as electron paramagnetic [13] properties of $SrTiO_3$.

Numerous authors has found band gap of $SrTiO_3$ has 3.25 eV experimentally [14,15]. However, the value of the band gap of STO calculated from DFT techniques was found to be 1.86 eV, 1.92eV and 1.63eV using QE, ABINT and WIEN2K code respectively [9,16-17]. The band gap energy of 2.7eV have been achieved by using Tran and Blaha modified Becke_Johnson (TB-mBJLDA) potential [18] using WIEN2K code [17]. Kinaci et al., (2010) used different exchange correlation functions such as PBE-GGA, LDA and LDA+U (U= 3.2, 5), resulting band gap of; 1.855, 1.717, 2.026 and 2.351 respectively, using VASP code [7]. The results of DFT, DFT + U, and TB-mBJLDA shown the calculated band gaps were underestimated compared to experimental value. So in this project, we calculates the band gap of STO using DFT, DFT+U with calculated U from linear response theory and DFT+U with incremental U methods in an attempt to find the best method for finding the band gap value that are much closer to the experimental measurement.

2.0 Computational Work

First-principles calculations based on DFT and DF+U were used for electronic properties calculation of STO as implemented in QUANTUM ESPRESSO (QE) package.

The calculation involved exchange and correlations according to local density approximation (LDA) function as parametrized by Perdew and Wang (PW91) pseudopotential. Computation were performed by chosen Ti site as origin of the cell and Sr at the body-center (0.5, 0.5, 0.5) with the three O atoms at the three face centers (0.5, 0.5, 0.0), (0.0, 0.5, 0.5) and (0.5, 0.0, 0.5) [19]. The lattice constant of 0.3905nm were adopted, from the experimental results [20]. From five-atom primitive unit cell of STO, supercell of 60 atoms were constructed by expanded unit cell (2 x 2 x 3 dimension).

First Brillouin zone of the material was accomplished using 6 x 6 x 4 points from Monkhorst-Pack method [19]. Energy cutoff of 90 Rydberg in a plane-wave basis set was used for calculation. Marzari-Vanderbilt smearing size was fixed to 0.1 Ry. Geometry optimization of the supercell were performed using variable cell relaxation (vc-relax) calculation as implemented in Quantum Espresso code. Three different methods were adopted for calculating electronic properties of STO: DFT without U value (method 1), DFT+U with calculated U (method 2) and DFT+U with incremented U (method 3). The calculated Hubbard U was determined using linear response theory. For incremented U, seven U values were used starting from 4.27 to 10.27 with an interval of 1, where band gap value will be determined from the calculated band structure with changing in U. The band gap values from the three methods will be compared and hence will determine the best method for finding the band gap for $SrTiO_3$ using first principle methods.

3.0 Results and discussions

Table 1, shows the result of value of band gap of $SrTiO_3$ calculated using DFT, DFT+U with linear response and DFT+U with incremental method. Our calculated band gap of STO using DFT was 1.85 eV which is in good agreement with earlier DFT calculations [7, 9,16-17]. For DFT+U with calculated U, the U value were obtained using linear response theory was 3.27 which resulted to calculated band gap of 2.19 eV. Figure 1 shows the graph of bandgap value versus Hubbard U for DFT+U with incremental U. Here, the band gap values increases with increasing the U value from 4.27 to 8.27 which later decreases until U=10.27. The band gap value of 2.43 eV and 3.06 eV were obtained from U of 4.27 and 8.27 respectively, while bandgap value of 2.19 eV was obtained at U of 10.27. For DFT+U with incremental U, the maximum band gap of 3.06 eV was found at 8.27 of U. Our results obtained using standard PW91 exchange correlation potential is found to be closed to

experimentally determined indirect band gap value of 3.25eV. Similar result was reported by Wahl, Vogtenhuber, & Kresse, (2008), with band gap value of 3.07 eV, but they calculated their band structure using hybrid HSE06 exchange correlation functional using DFT method [21]. Our calculation shown that DFT+U with standard LDA can get results with agreement with DFT with hybrid functional.

	U value	Band Gap (eV)
DFT	-	1.85
DFT+U (using linear response theory for calculating U)	3.27	2.19
DFT+U (Incremental of U parameter)	4.27	2.43
	5.27	2.58
	6.27	2.74
	7.27	2.96
	8.27	3.06
	9.27	2.68
	10.27	2.19

Table 1: The value of band gap of $SrTiO_3$ calculated using DFT and DFT+U

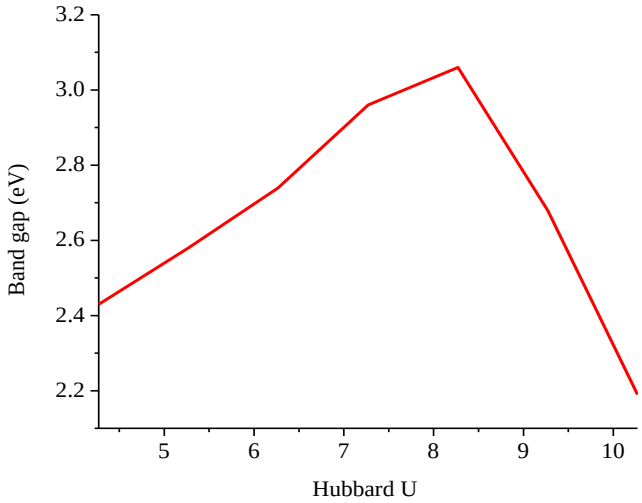

Figure 1: Trend of Hubbard U parameter on the energy band gap of $SrTiO_3$

3.1. Band Structure

The band gap data in table 1 was measured from band structure shows in figure 2. In this figure, the band structure of $SrTiO_3$ were calculated with high symmetry lines along the Brillouin zone paths; R (0.5 0.5 0.5), Γ (0.0 0.0 0.0), X (0.0 0.5 0.0) and M (0.5 0.5 0.0). The valence band maximum (VBM) and the conduction band minimum (CBM) lies at Γ point of the electronic band structures for three methods indicate the direct band gap properties of material.

The maximum valence band region of all the samples that located at Γ point were composed of the O-2p states with a minor contribution of Ti-3d and Sr-4p states while the minimum conduction band region originated from 3d and 2p orbital states of Ti and O respectively. The Fermi energy level (E_f) are indicated with red line as shown in fig. 2. Our E_f were calculated to be; 5.7097 eV (method 1), 7.4364 eV (method 2) and 7.8524 eV (method

3). The E_f was found to be closed to VBM by using method 1 which indicates p-type material. Using method 2 and 3, the E_f was found closed to CBM which shows n-type of the materials and is in good agreement with experimental result [7,22].

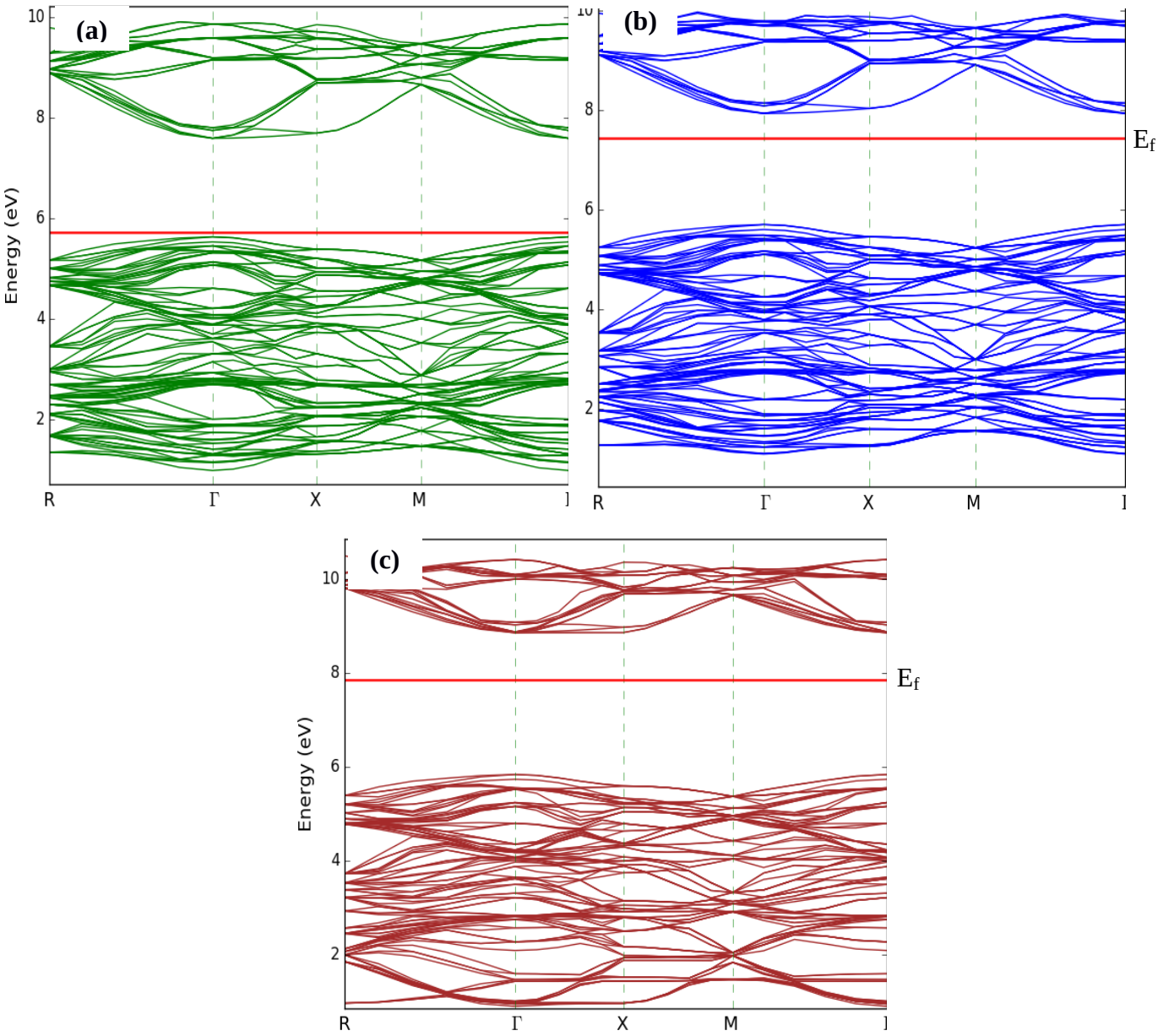

Figure 2: Band structure of STO using; (a) DFT, (b) DFT+U with calculated U. and (c) DFT+U with incremental U, along the symmetry line of Brillouin zone. The energy scale is in atomic units and red line indicate the Fermi level

3.3 Density of state

In Figure 3, total density of states show the region of conduction and valence band with vertical dotted line which indicate Fermi level (E_f) on energy scale. Similar to the band structures, the three density of states calculated from three methods are similar in the shape of density of states below and above the Fermi level. The density of states plots only differ in the width of the gap at the Fermi level, as indicated from the increasing value of band gap from band structure calculations. However close inspection shows that the peaks at the valence band (VB) are more pronounced in the density of state plot by DFT+Us' calculations.

Figure 3 also shows that the energy difference of VB to E_f are 0.99, 2.68 and 3.02 eV with intensity of the peak values of 74.5, 75.2 and 77.8 for method 1, 2 and 3 respectively. Likewise, the energy difference of conduction band (CB) from E_f are 3.80, 2.32 and 2.28 eV with intensity of the peak values at 64, 71 and 58.6 for method 1, 2 and 3 respectively. Fermi level shifted to level near in method 3 indicates the n type material as discussed in the previous paragraph.

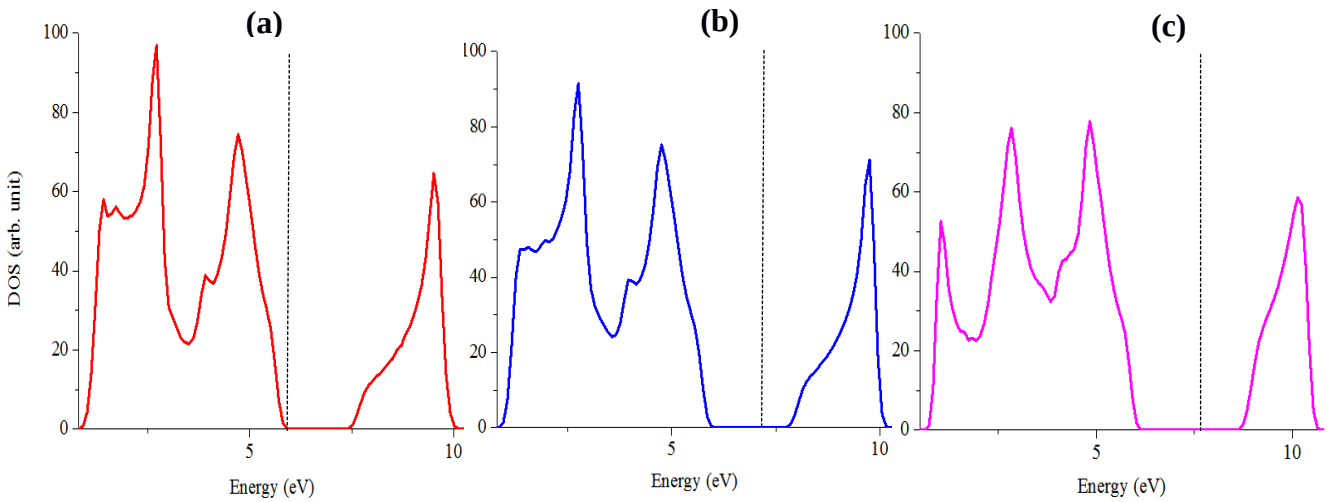

Figure 3: Total density of state of STO using (a) DFT, (b) DFT+U with calculated U and (c) DFT+U with incremental U methods.

The plots of partial density of states calculated using DFT, DFT+U with calculated U and DFT+U with incremental U values were shown in Figure 4. These plots are used to shows the participation of different atoms in the band structure with their possible linear

combination of atomic orbitals. The top of valence band region is mainly dominated by 2p orbital of O with a small contribution of 3d and 4p orbitals of Ti and Sr respectively, while the conduction band region is formed mainly by the 3d states of Ti with some part of the 2p states of O. The valence states are dominated by the 2p orbital of O and the 3d orbital of Ti which is 3.018 eV to the Fermi level. Intensity of DOS of Ti-3d orbital are pronounced in VB towards the core in methods 3 compared to 1and 2 methods. There are also some changes in shapes of DOS of O-2p orbital from method 1,2 and 3, whereas in method 3 the three peaks of the DOS of O-2p orbital are more pronounced compared to other two methods.

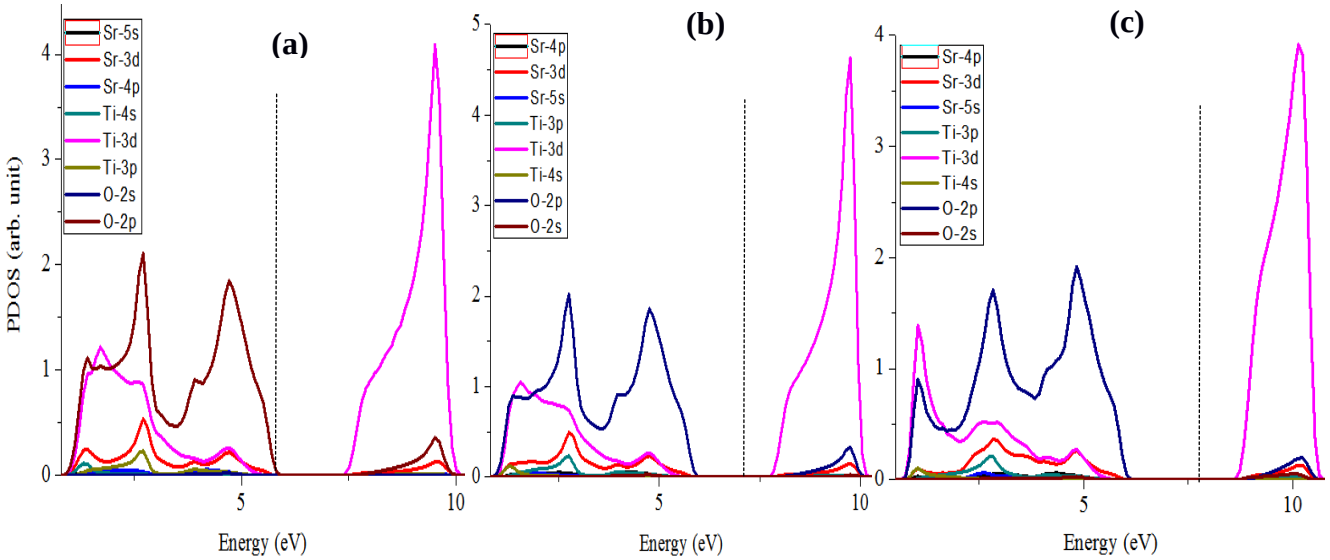

Figure 4: Partial density of state (PDOS) of STO using (a) DFT, (b) DFT+U with calculated U and (c) DFT+U with incremental U methods.

4 Conclusions

From our calculations, the value of the $SrTiO_3$ band gap of 1.8 eV from DFT technique, which is much lower than the experimental value, can be improved by using DFT+U with incremental value of U parameters, which is 3.06 eV that is closed to experimental result of 3.25 eV. DFT+U with calculated U parameter, only offered slightly higher value of band gap at 2.19 eV. The addition of parameter Hubbard U in DFT calculations did not have any influence in the shape of the total density of states but did changed the shapes of the partial density of states especially in the shape of DOS of Ti-3d and O-2p orbitals. The Fermi level shifted up from closer to the valence band to closer to the conduction band as in DFT+U calculation of $SrTiO_3$ which lead to changes in material electronic type.

Acknowledgements

The authors would like to thank Center of Excellence Frontier Materials Research, Center of Excellence Geopolymer and Green Technology (CEGeoGTech), the School of Materials Engineering, Universiti Malaysia Perlis and Malaysian Government for financing this project through the Fundamental Research Grant Scheme (FRGS/1/2016/STG07/UNIMAP/02/3).

References

1. Himmetoglu, B., Floris, A., Gironcoli, S., & Cococcioni, M. (2014). Hubbard-corrected DFT energy functionals: The LDA+ U description of correlated systems. *International Journal of Quantum Chemistry*, *114*(1), 14-49.
2. Tran, F., & Blaha, P. (2017). Importance of the Kinetic Energy Density for Band Gap Calculations in Solids with Density Functional Theory. J. Phys. Chem. A, 121(17), 3318-3325.
3. Yang, Z. H., Peng, H., Sun, J., & Perdew, J. P. (2016). More realistic band gaps from meta-generalized gradient approximations: Only in a generalized Kohn-Sham scheme. *Physical Review B*, *93*(20), 205205.
4. Yang, J., Tan, L. Z., & Rappe, A. M. (2017). Hybrid functional pseudopotentials. *arXiv preprint arXiv:1707.04501*.
5. Morales García, Á., Valero, R., & Illas, F. (2017). An empirical, yet practical way to predict the band gap in solids by using density functional band structure calculations. *The Journal of Physical Chemistry C*.

6. Parhizgar, S. S., & Beheshtian, J. (2018). Effect of nitrogen doping on electronic and optical properties of ZnO sheet: DFT+ U study. Computational Condensed Matter, 15, 1-6.
7. Kinaci, A., Sevik, C., & Çağın, T. (2010). Electronic transport properties of $SrTiO_3$ and its alloys: $Sr_{1-x}La_xTiO_3$ and $SrTi_{1-x}M_xO_3$ (M= Nb, Ta). *Physical Review B*, *82*(15), 155114.
8. Salehi, H. (2011). First Principles Studies on the Electronic Structure and Band Structure of Paraelectric $SrTiO_3$ by Different Approximations. *Journal of Modern Physics*, *2*(09), 934.
9. Mete, E., Shaltaf, R., & Ellialtıoğlu, Ş. (2003). Electronic and structural properties of a 4 d perovskite: cubic phase of SrZrO 3. Physical Review B, 68(3), 035119.
10. Breckenfeld, E., Wilson, R., Karthik, J., Damodaran, A. R., Cahill, D. G., & Martin, L. W. (2012). Effect of growth induced (non) stoichiometry on the structure, dielectric response, and thermal conductivity of $SrTiO_3$ thin films. *Chemistry of Materials*, *24*(2), 331-337.
11. Lee, C. H., Podraza, N. J., Zhu, Y., Berger, R. F., Shen, S., Sestak, M., Collins, R.W., Kourkoutis, L. F., Mundy, J.A., Wang, H & Mao, Q. (2013). Effect of reduced dimensionality on the optical band gap of $SrTiO_3$. *Applied Physics Letters*, *102*(12), 122901.
12. Monti, M., Sanz, M., Oujja, M., Rebollar, E., Castillejo, M., Pedrosa, F. J., Bollero, A., Camarero, J., Cunado, J. L. F., Nemes, N. M. & Mompean, F. J. (2013). Room temperature in-plane⟨ 100⟩ magnetic easy axis for $Fe_3O_4/SrTiO_3$ (001): Nb grown by infrared pulsed laser deposition. *Journal of Applied Physics*, *114*(22), 223902.
13. Azamat, D. V., Dejneka, A., Lancok, J., Trepakov, V. A., Jastrabik, L., & Badalyan, A. G. (2012). Electron paramagnetic resonance studies of manganese centers in $SrTiO_3$: Non-Kramers Mn^{3+} ions and spin-spin coupled Mn^{4+} dimers. *Journal of Applied Physics*, *111*(10), 104119.
14. Lobacheva, O., Yiu, Y. M., Chen, N., Sham, T. K., & Goncharova, L. V. (2017). Changes in local surface structure and Sr depletion in Fe-implanted SrTiO3 (001). Applied Surface Science, 393, 74-81.
15. Devi, L. G., & Anitha, B. G. (2018). Exploration of vectorial charge transfer mechanism in TiO2/SrTiO3 composite under UV light illumination for the degradation of 4-Nitrophenol: A comparative study with TiO2 and SrTiO3. Surfaces and Interfaces, 11, 48-56.
16. Shanmugapriya, K., Palanivel, B., & Murugan, R. (2017). Electronic and Thermoelectric Properties of SrTiO3. Current Smart Materials, 2(1), 73-79.
17. Sakhya, A. P., Maibam, J., Saha, S., Chanda, S., Dutta, A., Sharma, B. I., Thapa, R. K., & Sinha, T. P. (2015). Electronic structure and elastic properties of $ATiO_3$ (A= Ba, Sr, Ca) perovskites: A first principles study
18. Manzar, A., Murtaza, G., Khenata, R., & Muhammad, S. (2013). Electronic Band Profile and Optical Response of Spinel MgIn2O4 through Modified Becke—Johnson Potential. Chinese Physics Letters, 30(6), 067401.
19. Gallegos-Orozco, V., Martínez-Sánchez, R., & Espinosa-Magaña, F. (2008). In situ characterization of the ferroelectric transition in Ba Ti O 3 by EELS and comparison with ab initio methods. Physical Review B, 77(4), 045128.
20. Moure, C., & Peña, O. (2015). Recent advances in perovskites: Processing and properties. *Progress in Solid State Chemistry*, *43*(4), 123-148.

21. Wahl, R., Vogtenhuber, D., & Kresse, G. (2008). SrTiO 3 and BaTiO 3 revisited using the projector augmented wave method: Performance of hybrid and semilocal functionals. Physical Review B, 78(10), 104116.
22. Maldonado, F., Maza, L., & Stashans, A. (2017). Electronic properties of Cr-, B-doped and codoped SrTiO3. Journal of Physics and Chemistry of Solids, 100, 1-8.